Key Points:
- This study explores why some historical El Niño events significantly increased rainfall in California but some other events did not
- Statistical data analyses and model experiments show that persistently warm far eastern Pacific excites an optimal stationary wave pattern
- During the last 69 years, only three such events have occurred, which explains the fragile relationship between El Niño and California rainfall

On the Fragile Relationship Between El Niño and California Rainfall

Sang-Ki Lee[1] [iD], **Hosmay Lopez[2,1]**, **Eui-Seok Chung[3]** [iD], **Pedro DiNezio[4]** [iD], **Sang-Wook Yeh[5]** [iD], and **Andrew T. Wittenberg[6]** [iD]

[1]NOAA Atlantic Oceanographic and Meteorological Laboratory, Miami, FL, USA, [2]Cooperative Institute for Marine and Atmospheric Studies, University of Miami, Miami, FL, USA, [3]Rosenstiel School of Marine and Atmospheric Science, University of Miami, Miami, FL, USA, [4]Institute for Geophysics, University of Texas at Austin, Austin, TX, USA, [5]Department of Marine Sciences and Convergent Technology, Hanyang University, Ansan, South Korea, [6]NOAA Geophysical Fluid Dynamics Laboratory, Princeton, NJ, USA

Abstract The failed influence of the 2015–2016 El Niño on California rainfall has renewed interest in the relationship between El Niño and U.S. rainfall variability. Here we perform statistical data analyses and simple model experiments to show that sufficiently warm and persistent sea surface temperature anomalies (SSTAs) in the far eastern equatorial Pacific are required to excite an anomalous cyclone in the North Pacific that extends to the east across the U.S. West Coast and thus increases rainfall over California. Among the four most frequently recurring El Niño patterns considered in this study, only the persistent El Niño, which is often characterized by the warm SSTAs in the far eastern equatorial Pacific persisting throughout the winter and spring, is linked to such extratropical teleconnection patterns and significantly increased rainfall over the entire state of California. During the last 69 years, only three of the 25 El Niño events (i.e., 1957–1958, 1982–1983, and 1997–1998) are clearly identified as the persistent El Niño. In addition, the monthly rainfall variance explained by El Niño is less than half that caused by internal variability during the 25 El Niño. Therefore, the rarity of persistent El Niño events combined with the large influence of internal variability effectively explains the fragile relationship between El Niño and California rainfall.

1. Introduction

During El Niño winter and spring, the atmospheric jet stream over the northeast Pacific strengthens toward North America often increasing rainfall across the state of California, northern Mexico, and southern United States (e.g., Hoell et al., 2016; Jong et al., 2016; Krishnamurthy et al., 2015; Lee, Mapes, et al., 2014; Mo, 2010; Ropelewski & Halpert, 1986). Indeed, California experienced the wettest winter and spring (January–May; JFMAM) during the 1997–1998 El Niño (2.91 mm d^{-1}) since 1948 and the third wettest during the 1982–1983 El Niño (2.43 mm d^{-1}). Therefore, when the sea surface temperature anomalies (SSTAs) in Niño 3.4 (120°W–170°W and 5°S–5°N) reached a record high value in November 2015, it was highly anticipated that the 2015–2016 El Niño could end the most severe multiyear drought ever recorded in the state of California (Diaz & Wahl, 2015; Griffin & Anchukaitis, 2014; Seager et al., 2015). By some measures, the 2015–2016 El Niño (Figure 1c) did become the strongest El Niño yet recorded (L'Heureux et al., 2017) and caused a wide range of climate extremes around the globe (Mekonnen et al., 2016, 2017). However, California experienced only slightly above-normal winter and spring rainfall, mostly in the northern watershed regions (Figure 1f).

A plausible cause for the failed influence of the 2015–2016 El Niño on California rainfall is subseasonal atmospheric variability, such as the Pacific-North American pattern, the North Pacific Oscillation, and the Arctic Oscillation, which could disrupt the stationary Rossby wave trains emanating from the equatorial Pacific (e.g., Cohen et al., 2017; Deser et al., 2017; Hoerling & Kumar, 1997; Lin et al., 2017; Linkin & Nigam, 2008; Teng & Branstator, 2017; Wang et al., 2017). This hypothesis is supported by the marginal correlation between the Niño 3.4 SSTAs and California rainfall in JFMAM ($r = 0.36$, statistically significant at the 5% level).

El Niño intensity is also an important factor (e.g., Hoell et al., 2016; Jong et al., 2016). Hoell et al. (2016) used a multimodel ensemble of historical climate simulations to show that the odds for wet conditions significantly increase across the entire state only during strong El Niño events. However, this notion of El Niño intensity controlling the California rainfall response apparently did not apply to the 2015–2016 El Niño, which was a very strong event with its Nino3.4 SSTA in JFMAM (1.7°C) comparable to that during the 1982–1983 (1.7°C) and 1997–1998 (1.6°C) events (Figures 1a–1c).
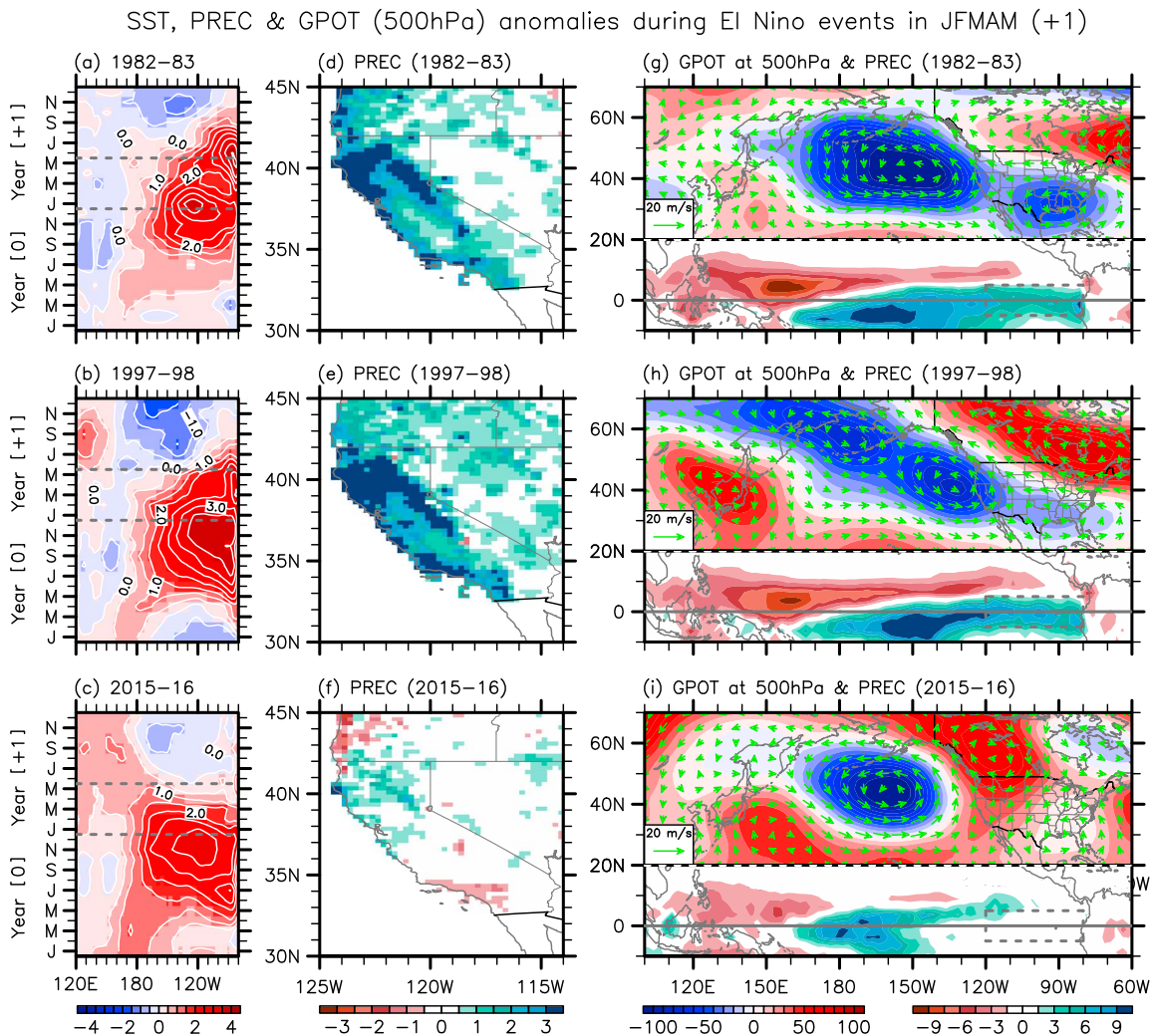
Figure 1. (a–c) Time-longitude plots of the tropical Pacific SSTAs averaged between 5°S and 5°N, JFMAM(+1)-averaged (d–f) rainfall anomalies over California, (g–i) rainfall anomalies over the tropical Pacific, and geopotential height and wind vector anomalies at 500 hPa for the 1982–1983 (Figures 1a, 1d, and 1g), 1997–1998 (Figures 1b, 1e, and 1h), and 2015–2016 El Niño events (Figures 1c, 1f, and 1i). The dashed gray lines in Figures 1a–1c indicate January 1(+1) and May 31(+1). The dashed gray boxes in Figures 1g–1i indicate the eastern equatorial Pacific (120°W–80°W and 5°S–5°N). The units are °C for SSTAs, mm d^{-1} for rainfall, gpm for geopotential height, and m s^{-1} for wind vectors.

Another important factor is the spatial pattern of El Niño, which can differ widely from event to event (Capotondi et al., 2015). Chiodi and Harrison (2013) showed that El Niño's teleconnections to the United States stem from those events that strongly affect atmospheric deep convection over the eastern tropical Pacific. Jo et al. (2015) showed that the equatorial Pacific warm SSTAs and the Aleutian low-pressure anomalies associated with El Niño–Southern Oscillation (ENSO) had shifted westward since the 1998–1999 regime shift, which could potentially weaken the relationship between El Niño and California rainfall. In line with this hypothesis, Paek et al. (2017) showed that the tropical Pacific SSTAs during the 2015–2016 event were displaced farther to the west and thus forced stationary Rossby wave trains different from those during the 1982–1983 and 1997–1998 events.

As briefly summarized above, previous studies have shown that the relationship between El Niño and California rainfall is quite fragile. In fact, if the 1982–1983 and 1997–1998 events are removed from the time series, the correlation between the Niño 3.4 SSTAs and California rainfall in JFMAM reduces to only 0.23, which is statistically insignificant at the 5% level based on a Student's *t* test—all statistical tests in this study are two tailed and use the number of observations as the degrees of freedom. Therefore, an important question arises as to what are the ingredients critical for the significantly enhanced California rainfall in the 1982–1983 and 1997–1998 events but missing in some other El Niño events. To address this question, we

first examine the 1982–1983, 1997–1998, and 2015–2016 El Niño events to build a hypothesis that the far eastern equatorial Pacific (i.e., east of around 120°W) warm SSTAs should persist throughout boreal winter and spring to significantly enhance rainfall across the state of California. To test this hypothesis, we explore the sensitivity of California rainfall to various flavors of El Niño. First, we briefly summarize the four most frequently recurring spatiotemporal patterns of El Niño (Lee, DiNezio, et al., 2014). Then, we present statistical analyses that link the four El Niño patterns to the tropical Pacific rainfall, extratropical stationary Rossby wave trains and California rainfall. We also present simple model experiments to further illustrate how the far eastern equatorial Pacific warm SSTAs could play a critical role in modulating the pathway of stationary Rossby wave trains toward North America.

2. Data, Methods, and Model

The Extended Reconstructed SST version 5 is used to compute the equatorial Pacific SSTAs for the period of 1949–2016 (Huang et al., 2017). The Climate Prediction Center (CPC) unified gauge-based analysis of the U.S. daily precipitation is used to derive monthly rainfall anomalies over the United States for 1949–2016 (Higgins et al., 1996). The CPC-Merged Analysis of Precipitation is used to derive rainfall anomalies over the tropical Pacific for 1979–2016 (Xie & Arkin, 1997). The NCEP-NCAR reanalysis for the period of 1949–2016 is used to derive geopotential height and wind anomalies (Kalnay et al., 1996).

To objectively characterize the spatiotemporal evolution of equatorial Pacific SSTAs during El Niño events, we follow the method presented in Lee, DiNezio, et al. (2014) using the linearly detrended global SSTAs. First, we identify 25 El Niño events for the period of 1948–2016 based on the threshold that the 3 month averaged SSTAs in Niño 3.4 is equal to or higher than 0.5°C for at least five consecutive months. Then, for each individual event, we construct longitude-time maps of SSTAs averaged in the equatorial Pacific between 5°S and 5°N. The longitude axis spans the entire equatorial Pacific (120°E–80°W), while the time axis is from January of the onset year to December of the decay year; hereafter, the suffix(0) indicates any month in an ENSO onset year, whereas the suffix(+1) any month in an ENSO decay year. Then, we use these 25 longitude-time maps of equatorial Pacific SSTAs to carry out an empirical orthogonal function (EOF) analysis to identify the preferred spatiotemporal modes of inter-El Niño variability. Next, the rainfall anomalies over the tropical Pacific and the state of California, and the geopotential height and wind anomalies at 500 hPa are regressed on the leading modes of inter-El Niño variability to examine the relationship between inter-El Niño variations and California rainfall.

We also use a simple two-level stationary wave model (Lee et al., 2013, 2009) to better understand how different El Niño flavors modulate the pathways of stationary Rossby wave trains toward North America. The simple model is a steady state primitive equation model, linearized with respect to specified background flow and driven by diabatic heating anomalies at 500 hPa.

The wet season for the state of California is between November and April. However, the correlation between the Niño 3.4 SSTAs and California rainfall is largest during JFMAM and very weak in November and December (e.g., Jong et al., 2016); thus, we focus on JFMAM throughout this study.

3. The 1982–1983, 1997–1998, and 2015–2016 El Niño Events

As shown in Figures 1a and 1b, the spatiotemporal patterns of the equatorial Pacific SSTAs during the 1982–1983 and 1997–1998 events are quite similar. In particular, during both events the warm SSTAs in the far eastern equatorial Pacific persist throughout JFMAM(+1). During the 2015–2016 event, however, the warm SSTAs in the far eastern equatorial Pacific dissipate relatively quickly after the peak season and disappear after around March(+1). In line with these SSTA patterns, the tropical Pacific rainfall anomalies in JFMAM(+1) are extended to the west coast of South America during the 1982–1983 and 1997–1998 events but confined to the west of 120°W during the 2015–2016 event (Figures 1g–1i). As also shown in Figures 1g–1i, the associated deep tropical convection anomalies force stationary Rossby wave trains that in turn strengthen the Aleutian low pressure system (i.e., an anomalous cyclone in the North Pacific). During the 1982–1983 and 1997–1998 events, the anomalous cyclone in the North Pacific expands eastward across the U.S. West Coast, increasing rainfall over California. During the 2015–2016 event, however, the anomalous cyclone remains within the North Pacific and thus has little impact on rainfall over California.

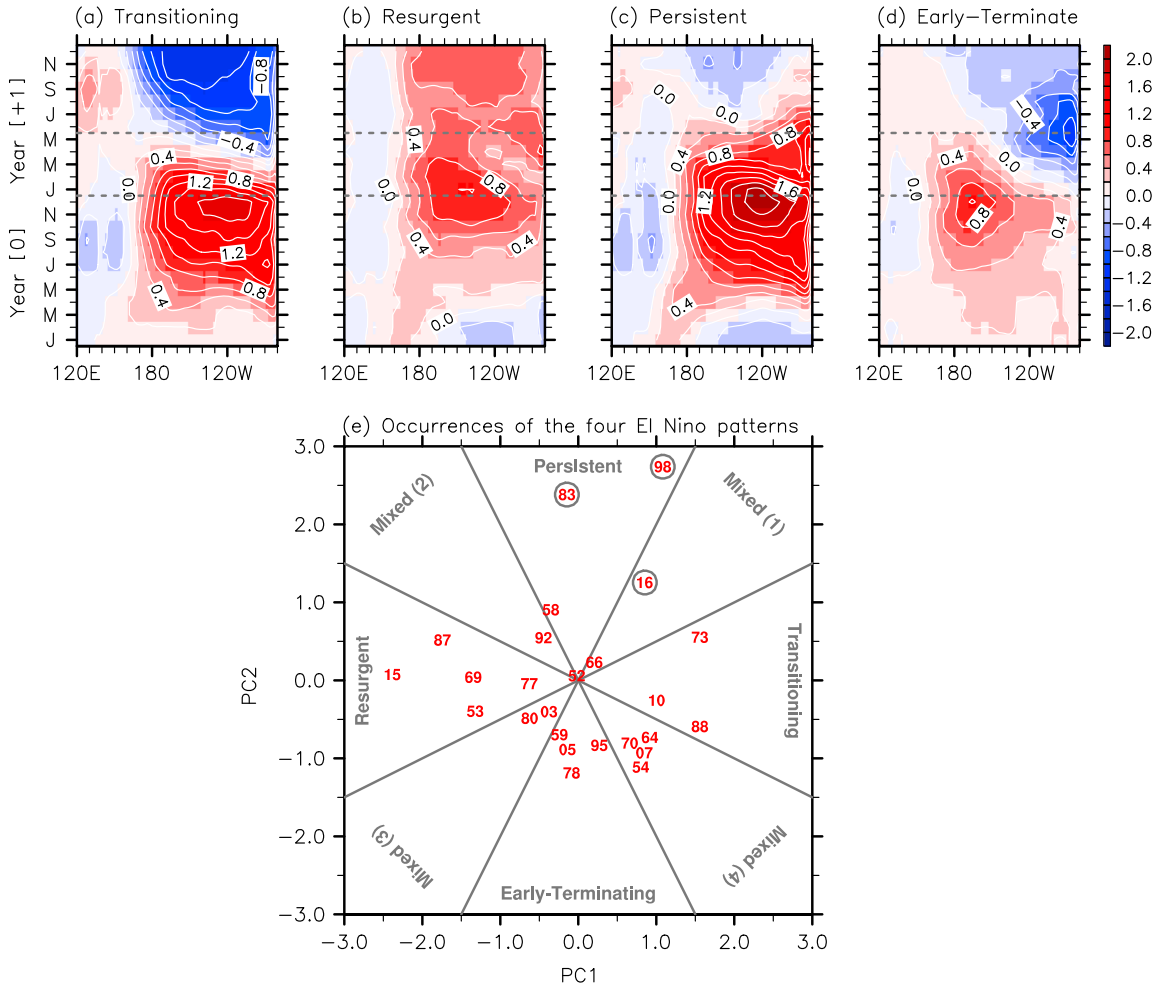Four most frequently recurring El Nino patterns & their occurrences

Figure 2. (a–d) Time-longitude plots of the tropical Pacific SSTAs, averaged between 5°S and 5°N, illustrate the four most frequently recurring El Niño patterns during 1948–2016, namely, (a) the transitioning, (b) resurgent, (c) persistent, and (d) early-terminating El Niño. (e) Normalized PC1 versus PC2 values for all 25 El Niño events. The two digit numbers indicate the El Niño decay years. The dashed gray lines in Figures 2a–2c indicate January 1(+1) and May 31(+1). The thick gray lines in Figure 2e are the boundaries (i.e., PC1 = ±2 × PC2 and PC2 = ±2 × PC1) that separate the four El Niño flavors from the mixed flavors. The units for SSTAs in Figures 2a–2d are in °C.

Based on the above analysis of the three El Niño events, it is logical to hypothesize that the warm SSTAs in the far eastern equatorial Pacific must persist throughout boreal winter and spring for the Aleutian low pressure system to extend eastward across the U.S. West Coast, which could in turn significantly enhance rainfall across the state of California. We will further explore this hypothesis in the next sections by investigating the four frequently recurring flavors of El Niño and their impacts on the tropical Pacific rainfall, extratropical stationary Rossby wave trains, and California rainfall.

4. Four Most Frequently Recurring El Niño Patterns

As summarized in section 2, Lee, DiNezio, et al. (2014) presented a new method to objectively characterize the spatiotemporal evolution of equatorial Pacific SSTAs during El Niño events. Applying this method to the historical El Niño events during 1949–2016, two leading orthogonal modes are obtained. The first and second modes explain about 37% and 25% of the interevent variance, respectively. Figures 2a and 2b show the composite mean anomalies of all 25 El Niño events plus and minus the first EOF mode, respectively. As summarized in these figures, the first mode distinguishes an early onset El Niño that transitions into La Niña (i.e., transitioning El Niño) from a late onset El Niño that returns for a consecutive year (i.e., resurgent El Niño).

Three El Niño events (1972–1973, 1987–1988, and 2009–2010) can be considered as early onset and transitioning, and five other El Niño events (1952–1953, 1968–1969, 1976–1977, 1986–191987, and 2014–1915) are examples of late onset and resurgent El Niño (Figure 2e).

Figures 2c and 2d show the composite mean anomalies of the 25 El Niño events plus and minus the second EOF mode, respectively. As shown in these figures, the second mode distinguishes a strong El Niño that persists in the far eastern equatorial Pacific throughout the winter and spring (i.e., persistent El Niño) from a weak El Niño that terminates early and promotes cold SSTAs in the far eastern equatorial Pacific after the peak season (i.e., early-terminating El Niño). Three El Niño events (1957–1958, 1982–1983, and 1997–1998) are examples of strong and persistent El Niño, and four other El Niño events (1958–1959, 1977–1978, 1994–1995, and 2004–2005) can be considered as weak and early terminating El Niño (Figure 2e).

Some El Nino events cannot be represented by only one of the four flavors. For example, four El Niño events (1953–1954, 1963–1964, 1969–1970, and 2006–2007) transitioned to La Niña events (i.e., transitioning El Niño) and their warm SSTAs in the far eastern Pacific dissipated prematurely (i.e., early-terminating El Niño). As such, the spatiotemporal evolution in each of the four mixed flavors (Figure 2e) is simply the linear combination of that between the two neighboring principal El Niño flavors as shown in Figure S1 in the supporting information. The 2015–2016 event is another example of a mixed flavor represented by both persistent and transitioning El Niño flavors. However, the 2015–2016 event is unique because its spatiotemporal pattern (Figure 1c) does not show the key characteristics of the persistent El Niño flavor.

5. California Rainfall Anomalies Associated With the Four El Niño Patterns

Figures 3e–3l show the rainfall anomalies over California and the tropical Pacific, and the geopotential height and wind anomalies at 500 hPa regressed on the leading modes of inter-El Niño variability. The composite mean anomalies of these variables during the 25 El Niño events are added to the regressed fields. The black dots in Figures 3e–3h indicate that the regressed rainfall anomalies are statistically significant at the 5% level based on a Student's *t* test. As shown in Figures 2a and 3a, a transitioning El Niño is characterized by a rapid transition of the warm SSTAs to the cold SSTAs in the far eastern equatorial Pacific during JFMAM(+1). The tropical Pacific rainfall anomalies associated with the transitioning El Niño are largely confined to the west of about 120°W. This is due to the lack of persistence in the far eastern equatorial Pacific warm SSTAs as shown in Figures S2i and S3i in the supporting information. The associated deep tropical convection anomalies produce an anomalous cyclone in the North Pacific that barely extends to the U.S. West Coast. As shown in Figure 3e, the transitioning El Niño is linked to above-normal rainfall in the northern and coastal regions of the state. However, this link exists only in JFM(+1) as shown in Figures S2e and S3e in the supporting information. A resurgent El Niño describes a relatively weak and late-onset El Niño that persists long and produces another El Niño event (Figures 2b and 3b). In this case, the warm SSTAs in the far eastern equatorial Pacific are typically not strong enough to produce deep tropical convection aloft. Similar to the transitioning El Niño, the anomalous cyclone in the North Pacific remains sufficiently far away from North America and thus has little influence on California rainfall.

As shown in Figures 2c and 3c, a persistent El Niño is characterized by the far eastern equatorial Pacific warm SSTAs persisting throughout JFMAM(+1). Consistently, the associated tropical Pacific rainfall anomalies are extended to the west coast of South America. In this case, the anomalous cyclone in the North Pacific extends farther eastward across the U.S. West Coast and is conjoined with another anomalous cyclone centered over the United States. Therefore, rainfall is significantly increased across the entire state throughout JFMAM(+1) as shown in Figure 3g (see also Figures S2g and S3g in the supporting information). An early-terminating El Niño is often characterized by a rapid emergence of cold SSTAs in the far eastern equatorial Pacific as early as January(+1) and relatively weak warm SSTAs in the central equatorial Pacific persisting in MAM(+1). Therefore, the associated tropical Pacific rainfall anomalies are mainly in the central tropical Pacific. In this case, the anomalous cyclone in the North Pacific stays completely away from North America and thus has little impact on California rainfall.

As shown in Figure S4 in the supporting information, the rainfall and atmospheric anomalies associated with each of the four mixed flavors are linear combinations of those between the two neighboring principal El Niño flavors. Therefore, the two mixed flavors neighboring the persistent El Niño flavor in Figure 2e are also linked to increased California rainfall. However, these mixed flavors do not always represent all characteristics
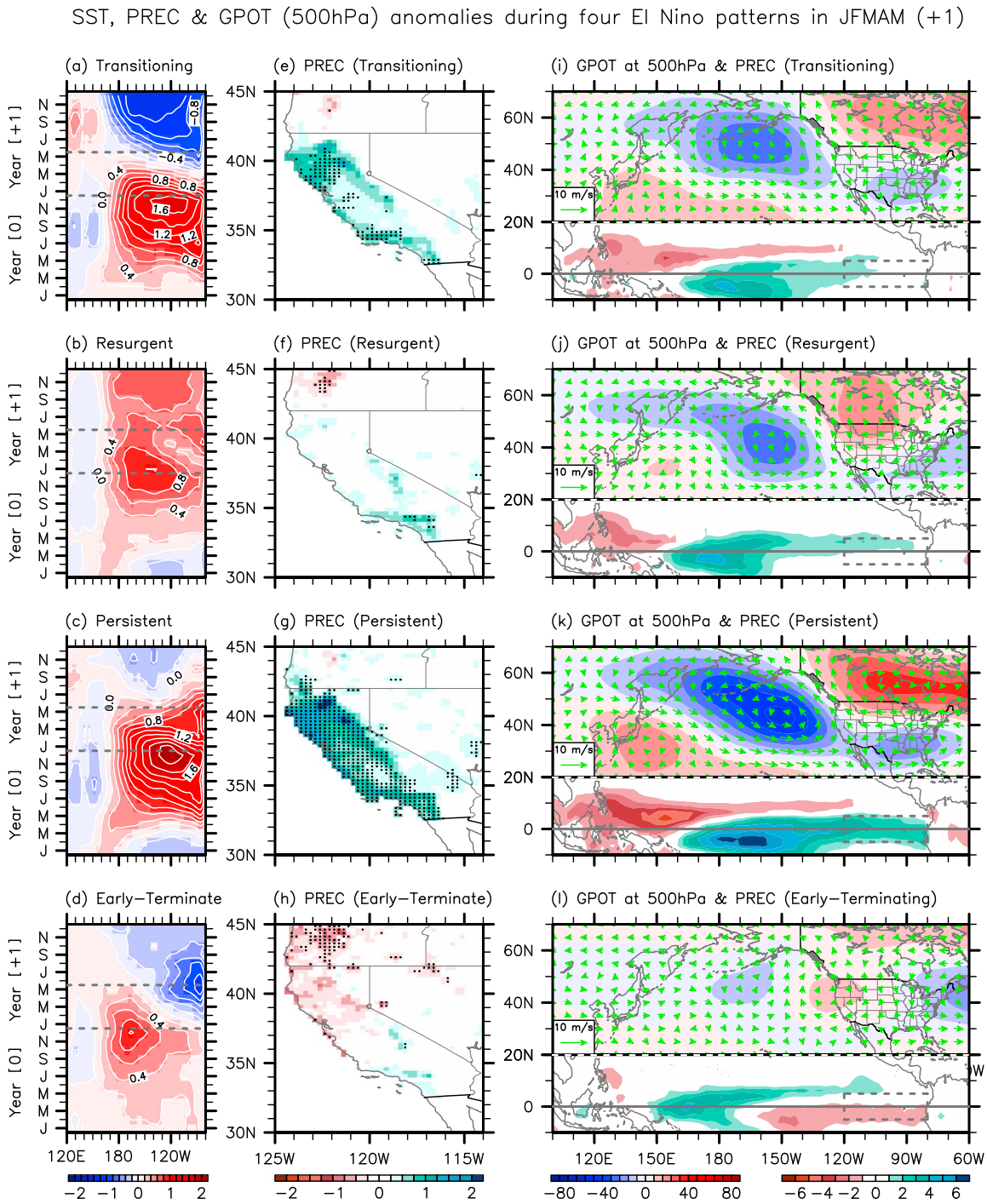
SST, PREC & GPOT (500hPa) anomalies during four El Nino patterns in JFMAM (+1)

Figure 3. (a–d) Time-longitude plots of the tropical Pacific SSTAs averaged between 5°S and 5°N, JFMAM (+1)-averaged (e–h) rainfall anomalies over California, (i–l) rainfall anomalies over the tropical Pacific, and geopotential height and wind vector anomalies at 500 hPa regressed on the transitioning (Figures 3a, 3e, and 3i), resurgent (Figures 3b, 3f, and 3j), persistent (Figures 3c, 3g, and 3k), and early-terminating El Niño (Figures 3d, 3h, and 3l). The dashed gray lines in Figures 3a–3d indicate January 1(+1) and May 31(+1). The dashed gray boxes in Figures 3i–3l indicate the eastern equatorial Pacific (120°W–80°W and 5°S–5°N). The units are °C for SSTAs, mm d^{-1} for rainfall, gpm for geopotential height, and m s^{-1} for wind vectors. The black dots in Figures 3e–3h indicate that the rainfall anomalies are statistically significant at the 5% level based on a Student's t test.

of the individual El Niño events. For instance, the 2015–2016 event is a mixed flavor of the persistent and transitioning El Niño. However, its spatiotemporal pattern does not show the key characteristics of the persistent El Niño flavor.
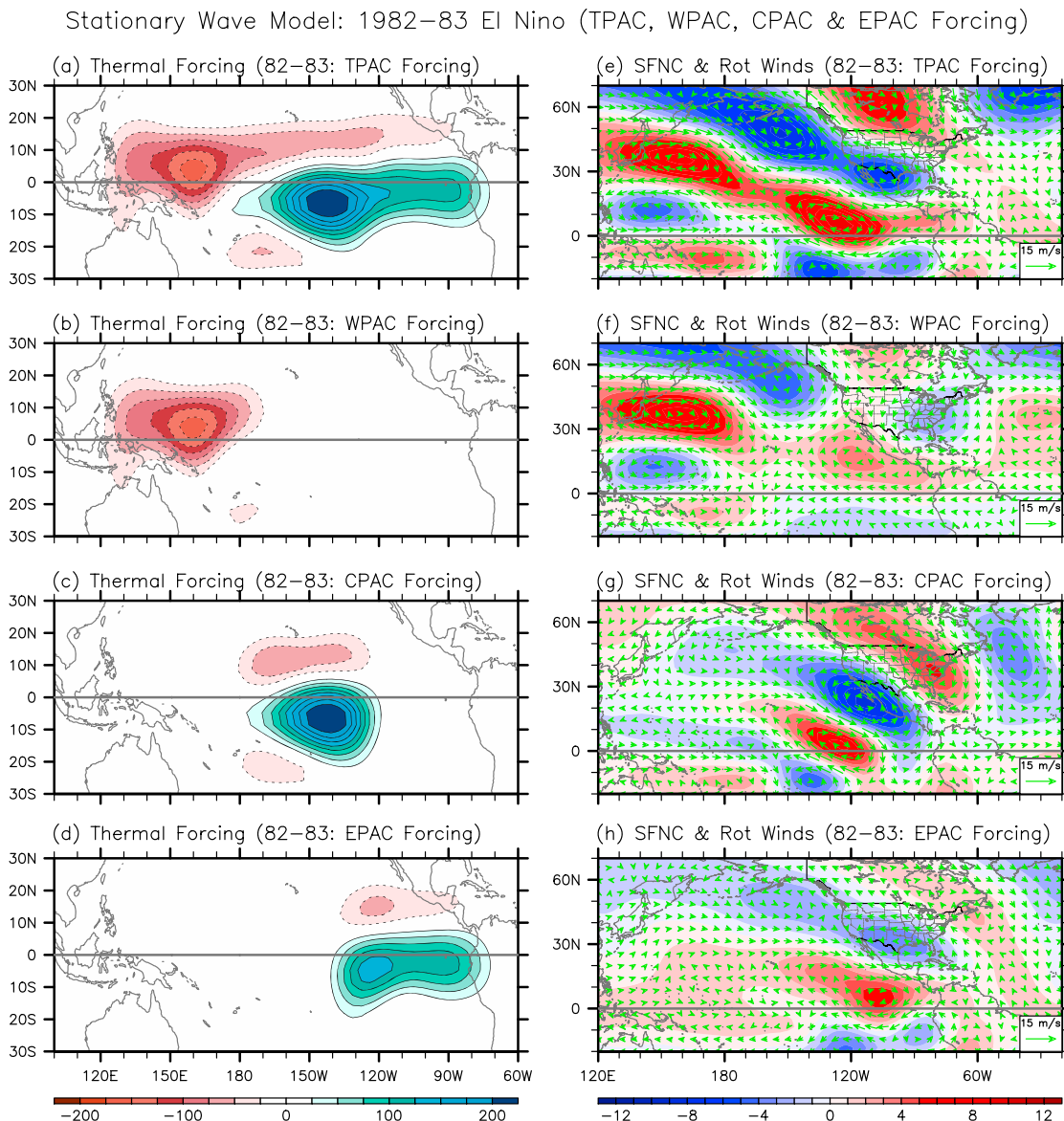
Figure 4. (a–d) Tropical Pacific heating anomalies prescribed (derived from the rainfall anomalies in JFMAM(+1) of the 1982–1983 El Niño) and (e–h) the corresponding barotropic stream function and rotational wind anomalies from the TPAC (Figures 4a and 4e), WPAC (Figures 4b and 4f), CPAC (Figures 4c and 4g), and EPAC experiments (Figures 4d and 4h). The units are W m^{-2} for thermal forcing, 10^6 m^2 s^{-1} for stream function, and m s^{-1} for wind vectors.

In summary, among the four El Niño flavors considered, only the persistent El Niño flavor produces an anomalous cyclone in the North Pacific that extends sufficiently eastward across the U.S. West Coast to significantly increase rainfall across the entire state of California. The other three El Niño flavors, which produce an anomalous cyclone that largely stays away from North America, have either limited influence in the northern and coastal regions of California or no influence at all.

However, it is important to note that the monthly rainfall variance explained by El Niño is less than half that caused by internal variability (i.e., signal-to-noise ratios <0.5) during the 25 El Niño events as shown in Figure S5 in the supporting information. This means that California rainfall during the four El Niño flavors can be greatly reduced or enhanced by internal variability in agreement with earlier studies (e.g., Deser et al., 2017).

6. Simple Model Experiments

To better illustrate how different spatial patterns of thermal forcing in the tropical Pacific modulate stationary wave trains toward North America, we performed four experiments using the simple two-level model. The

climatological winds in JFMAM at 250 and 750 hPa were derived from the NCEP-NCAR reanalysis and used as the background flows. In the first experiment (TPAC), the simple model was forced by the tropical Pacific (120°E–80°W and 20°S–20°N) heating anomalies in JFMAM(+1) of the 1982–1983 El Niño. The other three experiments are identical to the first experiment, except that the tropical Pacific heating anomalies of the 1982–1983 El Niño are confined to the western (120°E–180°; WPAC), central (180°–130°W; CPAC), and eastern (140°W–80°W; EPAC) tropical Pacific between 20°S–20°N. Figures 4a–4d show the tropical Pacific heating anomalies prescribed for the four experiments.

As shown in Figure 4e, the simple model reasonably well simulates the stationary Rossby wave trains emanating from the tropical Pacific during the 1982–1983 El Niño event (Figure 1g). In particular, the simulated anomalous cyclone in the North Pacific extends to the east across the U.S. West Coast and is conjoined with another anomalous cyclone centered over the United States as in the reanalysis (Figure 1g). If the heating anomalies are confined in the western tropical Pacific, an anomalous cyclone still forms in the North Pacific but is positioned too far north to affect the entire state of California (Figure 4f). When the model is forced by the central tropical Pacific heating anomalies, an anomalous cyclone forms in the northeast Pacific centered along the West Coast of United States and Mexico around 20°N. Lastly, when the simple model is forced in the eastern tropical Pacific, the anomalous cyclone in the North Pacific extends to the east across the U.S. West Coast and is conjoined with another anomalous cyclone centered over the United States. Therefore, the simple model experiments support the hypothesis that the far eastern equatorial Pacific warm SSTAs must persist throughout JFMAM(+1) to significantly enhance rainfall in the state of California.

7. Summary and Discussion

In this study, we explore the sensitivity of California's winter and spring rainfall to various flavors of El Niño. Among the four most frequently recurring spatiotemporal El Niño patterns considered, only the persistent El Niño, characterized by the far eastern equatorial Pacific warm SSTAs persisting throughout JFMAM(+1), significantly increases rainfall across the entire state of California. The associated anomalous cyclone in the North Pacific extends to the east across the U.S. West Coast and is conjoined with another anomalous cyclone centered over the United States. During the other three El Niño flavors, the anomalous cyclone largely stays away from North America and thus has either limited influence in the northern and coastal regions of the state or no influence at all.

Among the 25 El Niño events that occurred during 1948–2016, three events (i.e., 1957–1958, 1982–1983, and 1997–1998) are clearly identified as persistent El Niño events. During all these three events, rainfall over California greatly increased—California experienced the fifth wettest winter and spring during 1957–1958 El Niño (2.00 mm d^{-1}) since 1948. However, since only three such events occurred during the last 69 years, they are fairly rare events. Additionally, the signal-to-noise ratios rarely exceed 0.5 during the 25 El Niño events. Therefore, the rarity of persistent El Niño events combined with small signal-to-noise ratios effectively explains the fragile relationship between El Niño and California rainfall.

Some limitations in the statistical analysis should be pointed out. In particular, the lines that separate the four principal El Niño flavors from the mixed flavors in Figure 2e are somewhat arbitrary. The number of observed El Niño events considered (25 events) is also relatively small compared to the number of flavors (8 flavors), raising the possibility of overfitting to the available data.

There are many follow-up questions that require further investigations. One such question is whether the current state-of-the-art climate models reproduce the observed inter-El Niño variations related to the persistence (i.e., the second EOF mode). Yun et al. (2016) explored this question by looking at inter-El Niño variations in the Coupled Model Intercomparison Project phase 5 (CMIP5) models. They showed that a large portion of the CMIP5 models fall short in capturing the second EOF mode that distinguishes the persistent versus early-terminating El Niño, implying that some of the operational seasonal forecast models may suffer the same model deficiency. Finally, to further our study, future studies may examine the individual roles of spatial versus temporal aspects of various El Niño events using SST-forced atmospheric models.

References

Capotondi, A., Wittenberg, A. T., Newman, M., di Lorenzo, E., Yu, J. Y., Braconnot, P., … Yeh, S. W. (2015). Understanding ENSO diversity. *Bulletin of the American Meteorological Society*, *96*(6), 921–938. https://doi.org/10.1175/BAMS-D-13-00117.1

Chiodi, A. M., & Harrison, D. E. (2013). El Niño impacts on seasonal U.S. atmospheric circulation, temperature, and precipitation anomalies: The OLR-event perspective. *Journal of Climate*, *26*(3), 822–837. https://doi.org/10.1175/JCLI-D-12-00097.1

Cohen, J., Pfeiffer, K., & Francis, J. (2017). Winter 2015/16: A turning point in ENSO-based seasonal forecasts. *Oceanography*, *30*(1), 82–89. https://doi.org/10.5670/oceanog.2017.115

Deser, C., Simpson, I. R., McKinnon, K. A., & Phillips, A. S. (2017). The Northern Hemisphere extra-tropical atmospheric circulation response to ENSO: How well do we know it and how do we evaluate models accordingly? *Journal of Climate*, *30*(13), 5059–5082. https://doi.org/10.1175/JCLI-D-16-0844.1

Diaz, H. F., & Wahl, E. R. (2015). Recent California water year precipitation deficits: A 440-year perspective. *Journal of Climate*, *28*(12), 4637–4652. https://doi.org/10.1175/JCLI-D-14-00774.1

Griffin, D., & Anchukaitis, K. J. (2014). How unusual is the 2012–2014 California drought? *Geophysical Research Letters*, *41*(24), 9017–9023. https://doi.org/10.1002/2014GL062433

Higgins, R. W., Mo, K. C., & Schubert, S. D. (1996). The moisture budget of the central United States in spring as evaluated in the NCEP/NCAR and the NASA/DAO reanalyses. *Monthly Weather Review*, *124*(5), 939–963. https://doi.org/10.1175/1520-0493(1996)124%3C0939:TMBOTC%3E2.0.CO;2

Hoell, A., Hoerling, M., Eischeid, J., Wolter, K., Dole, R., Perlwitz, J., … Cheng, L. (2016). Does El Niño intensity matter for California precipitation? *Geophysical Research Letters*, *43*, 819–825. https://doi.org/10.1002/2015GL067102

Hoerling, M. P., & Kumar, A. (1997). Why do North American climate anomalies differ from one El Niño event to another? *Geophysical Research Letters*, *24*(9), 1059–1062. https://doi.org/10.1029/97GL00918

Huang, B., Thorne, P., Banzon, V., Boyer, T., Chepurin, G., Lawrimore, J., … Zhang, H. (2017). Extended reconstructed sea surface temperature version 5 (ERSSTv5): Upgrades, validations, and intercomparisons. *Journal of Climate*, *30*(20), 8179–8205. https://doi.org/10.1175/JCLI-D-16-0836.1

Jo, H.-S., Yeh, S.-W., & Lee, S.-K. (2015). Changes in the relationship in the SST variability between the tropical Pacific and the North Pacific across the 1998/99 regime shift. *Geophysical Research Letters*, *42*, 7171–7178. https://doi.org/10.1002/2015GL065049

Jong, B.-T., Ting, M., & Seager, R. (2016). El Niño's impact on California precipitation: Seasonality, regionality, and El Niño intensity. *Environmental Research Letters*, *11*(5), 054021. https://doi.org/10.1088/1748-9326/11/5/054021

Kalnay, E., Kanamitsu, M., Kistler, R., Collins, W., Deaven, D., Gandin, L., … Joseph, D. (1996). The NCEP/NCAR 40-year reanalysis project. *Bulletin of the American Meteorological Society*, *77*(3), 437–471. https://doi.org/10.1175/1520-0477(1996)077%3C0437:TNYRP%3E2.0.CO;2

Krishnamurthy, L., Vecchi, G. A., Msadek, R., Wittenberg, A., Delworth, T. L., & Zeng, F. (2015). The seasonality of the Great Plains low-level jet and ENSO relationship. *Journal of Climate*, *28*(11), 4525–4544. https://doi.org/10.1175/JCLI-D-14-00590.1

Lee, S.-K., DiNezio, P. N., Chung, E.-S., Yeh, S.-W., Wittenberg, A. T., & Wang, C. (2014). Spring persistence, transition and resurgence of El Niño. *Geophysical Research Letters*, *41*, 8578–8585. https://doi.org/10.1002/2014GL062484

Lee, S.-K., Mapes, B. E., Wang, C., Enfield, D. B., & Weaver, S. J. (2014). Springtime ENSO phase evolution and its relation to rainfall in the continental U.S. *Geophysical Research Letters*, *41*, 1673–1680. https://doi.org/10.1002/2013GL059137

Lee, S.-K., Mechoso, C. R., Wang, C., & Neelin, J. D. (2013). Interhemispheric influence of the northern summer monsoons on the southern subtropical anticyclones. *Journal of Climate*, *26*(24), 10193–10204. https://doi.org/10.1175/JCLI-D-13-00106.1

Lee, S.-K., Wang, C., & Mapes, B. E. (2009). A simple atmospheric model of the local and teleconnection responses to tropical heating anomalies. *Journal of Climate*, *22*(2), 272–284. https://doi.org/10.1175/2008JCLI2303.1

L'Heureux, M. L., Takahashi, K., Watkins, A. B., Barnston, A. G., Becker, E. J., Di Liberto, T. E., … Wittenberg, A. T. (2017). Observing and predicting the 2015–16 El Niño. *Bulletin of the American Meteorological Society*, *98*, 1363–1382. https://doi.org/10.1175/BAMS-D-16-0009.1

Lin, Y.-H., Hipps, L. E., Wang, S.-Y., & Yoon, J.-H. (2017). Empirical and modeling analyses of the circulation influences on California precipitation deficits. *Atmospheric Science Letters*, *18*(1), 19–28. https://doi.org/10.1002/asl.719

Linkin, M. E., & Nigam, S. (2008). The North Pacific Oscillation–west Pacific teleconnection pattern: Mature-phase structure and winter impacts. *Journal of Climate*, *21*(9), 1979–1997. https://doi.org/10.1175/2007JCLI2048.1

Mekonnen, A., Renwick, J. A., & Sanchez-Lugo, A. (Eds.) (2016). Regional climates [in "State of the. Climate in 2015"]. *Bulletin of the American Meteorological Society*, *97*(8), Si–S275. https://doi.org/10.1175/2016BAMSStateoftheClimate.1

Mekonnen, A., Renwick, J. A., & Sanchez-Lugo, A. (Eds.) (2017). Regional climates [in "State of the. Climate in 2016"]. *Bulletin of the American Meteorological Society*, *98*(8), Si–S280. https://doi.org/10.1175/2017BAMSStateoftheClimate.1

Mo, K. C. (2010). Interdecadal modulation of the impact of ENSO on precipitation and temperature over the United States. *Journal of Climate*, *23*(13), 3639–3656. https://doi.org/10.1175/2010JCLI3553.1

Paek, H., Yu, J.-Y., & Qian, C. (2017). Why were the 2015/2016 and 1997/1998 extreme El Niños different? *Geophysical Research Letters*, *44*, 1848–1856. https://doi.org/10.1002/2016GL071515

Ropelewski, C. F., & Halpert, M. S. (1986). North American precipitation and temperature patterns associated with the El Niño–Southern Oscillation (ENSO). *Monthly Weather Review*, *114*(12), 2352–2362. https://doi.org/10.1175/1520-0493(1986)114%3C2352:NAPATP%3E2.0.CO;2

Seager, R., Hoerling, M., Schubert, S., Wang, H., Lyon, B., Kumar, A., … Henderson, N. (2015). Causes of the 2011 to 2014 California drought. *Journal of Climate*, *28*(18), 6997–7024. https://doi.org/10.1175/JCLI-D-14-00860.1

Teng, H., & Branstator, G. (2017). Causes of extreme ridges that induce California droughts. *Journal of Climate*, *30*(4), 1477–1492. https://doi.org/10.1175/JCLI-D-16-0524.1

Wang, S., Anichowski, A., Tippett, M. K., & Sobel, A. H. (2017). Seasonal noise versus subseasonal signal: Forecasts of California precipitation during the unusual winters of 2015–2016 and 2016–2017. *Geophysical Research Letters*, *44*(18), 9513–9520. https://doi.org/10.1002/2017GL075052

Xie, P., & Arkin, P. A. (1997). Global precipitation: A 17-year monthly analysis based on gauge observations, satellite estimates, and numerical model outputs. *Bulletin of the American Meteorological Society*, *78*(11), 2539–2558. https://doi.org/10.1175/1520-0477(1997)078%3C2539:GPAYMA%3E2.0.CO;2

Yun, K.-S., Yeh, S.-W., & Ha, K.-J. (2016). Inter-El Niño variability in CMIP5 models: Model deficiencies and future changes. *Journal of Geophysical Research: Atmospheres*, *121*, 3894–3906. https://doi.org/10.1002/2016JD024964